When is the R = 1 epidemic threshold meaningful?

Kris V Parag[1,2,*], Anne Cori[1] and Uri Obolski[3,4]

[1]MRC Centre for Global Infectious Disease Analysis, Imperial College London, London, UK.

[2]NIHR HPRU in Behavioural Science and Evaluation, University of Bristol, Bristol, UK

[3]School of Public Health, Faculty of Medical & Health Sciences, Tel Aviv University, Tel Aviv, Israel.

[4]Porter School of the Environment and Earth Sciences, Faculty of Exact Sciences, Tel Aviv University, Tel Aviv, Israel.

*For correspondence: k.parag@imperial.ac.uk.

Abstract

The *effective reproduction number R* is a predominant statistic for tracking the transmissibility of infectious diseases and informing public health policies. An estimated *R=1* is universally interpreted as indicating epidemic stability and is a critical threshold for deciding whether new infections will grow ($R>1$) or fall ($R<1$). We demonstrate that this threshold, which is typically computed over coarse spatial scales, rarely signifies stability because those scales integrate infections from heterogeneous groups. Groups with falling and rising infections counteract and early-warning signals from resurging groups are lost in noisy fluctuations from stable groups with large infection counts. We prove that an estimated *R=1* is consistent with a vast space of epidemiologically diverse scenarios, diminishing its predictive power and policymaking value. We show that a recent statistic, *E*, derived from *R* via experimental design theory provides a more meaningful stability threshold (*E=1*) by rigorously constraining this space of scenarios.

Main

Accurately tracking the transmissibility of infectious diseases over time is a longstanding and important problem. Timely indicators of the growth or decline of epidemics contribute valuable evidence for informing public health policy, assessing interventions and improving epidemic response and pandemic preparedness [1]. The *effective reproduction number*, *R*, is the most commonly-used statistic for describing transmissibility and estimates the ratio of expected new infections to actively circulating (past) infections [2]. Although there are many approaches for computing *R* [3], its role as a threshold statistic is a fixture across epidemiology. An estimated *R=1* indicates that the incidence of new infections will remain roughly constant, while values above or below this threshold foretell of rising or falling incidence.

This interpretation is ubiquitous and its simplicity underlies why *R* is prominent as a predictive statistic for guiding public health responses and communicating the state of an epidemic [4]. However, as *R* is typically estimated from incidence data at a coarse spatial scale (usually nationally or regionally) [1], it regularly averages over groups with heterogeneous dynamics.

Consequently, finer scale variations containing critical signals for prediction and control are neglected. Group heterogeneities emerge from differences in behaviour, sociodemographic factors, immunity levels, location and other features [5,6]. Here we highlight how averaging over groups means that, even under the mildest assumptions, *R=1* seldom signifies epidemic stability. As a result, *R* may have substantial disadvantages as a prospective or retrospective statistic [7], especially at the large scales over which it is commonly inferred and reported.

To demonstrate these claims, consider *p>1* heterogeneous (but well-mixed) groups, with R_j as the reproduction number of group *j* and Λ_j as the infectious force in that group. The *R* that is frequently computed at regional or national scales is equivalent to a weighted mean:

$$R \stackrel{\text{def}}{=} \sum_{j=1}^{p} w_j R_j\,, \quad \text{with weights } w_j = \frac{\Lambda_j}{\sum_{i=1}^{p} \Lambda_i}. \quad (1)$$

The Λ_j are obtained by convolving past incident infections with the generation time distribution of the disease [2]. See the Supplement for more details on the equivalence between **Eq. (1)** and conventional formulae. Manipulating **Eq. (1)**, we find that any of the infinite solutions to $\sum_{j=1}^{p} \Lambda_j (R_j - 1) = 0$ satisfies the *R=1* threshold condition.

A vast space of epidemiologically diverse scenarios can yield *R=1*. At the simplest *p=2* setting, even if the mean $p^{-1}\sum_{j=1}^{p} R_j$ is 1 (the constraint in **Fig. 1)**, these scenarios include numerous solutions with $R_1>1$. This discordance between the interpretation of *R=1* and underlying group dynamics becomes harder to diagnose as *p* increases. **Fig. 1C** confirms this, exemplifying scenarios (with uncertainty) where multiple $R_j>1$ (and often no $R_j=1$) yet *R* still confidently signals epidemic stability. Such heterogeneity-driven discrepancies were frequently observed during the COVID-19 pandemic and Ebola virus epidemics [6,8–10].

How can we minimise this issue? A sensible approach might leverage information from the R_j to derive a global statistic *X* such that *X=1* does not conceal local or group-level signals of rising infections. One solution, $X = \max R_j$, guarantees this but is maximally conservative and sensitive to R_j estimate uncertainties. We generalise this solution by defining:

$$X(\gamma) \stackrel{\text{def}}{=} \sum_{j=1}^{p} \omega_j(\gamma) R_j\,, \quad \text{with weights } \omega_j(\gamma) = \frac{R_j^{\gamma}}{\sum_{i=1}^{p} R_i^{\gamma}}. \quad (2)$$

As γ increases, **Eq. (2)** interpolates between the group average $X(0) = p^{-1}\sum_{j=1}^{p} R_j$ and $X(\infty) = \max R_j$. If we can optimise γ, we should be able to balance between vulnerability to

false indication of stability, stemming from over-averaging, and overly conservative signalling. Experimental design theory was used in [10] to compute the weighting of R_j that minimises the maximum uncertainty across the R_j estimates. This yields the *risk-averse reproduction number E,* which within our framework of **Eq. (2)** satisfies $E = X(1)$.

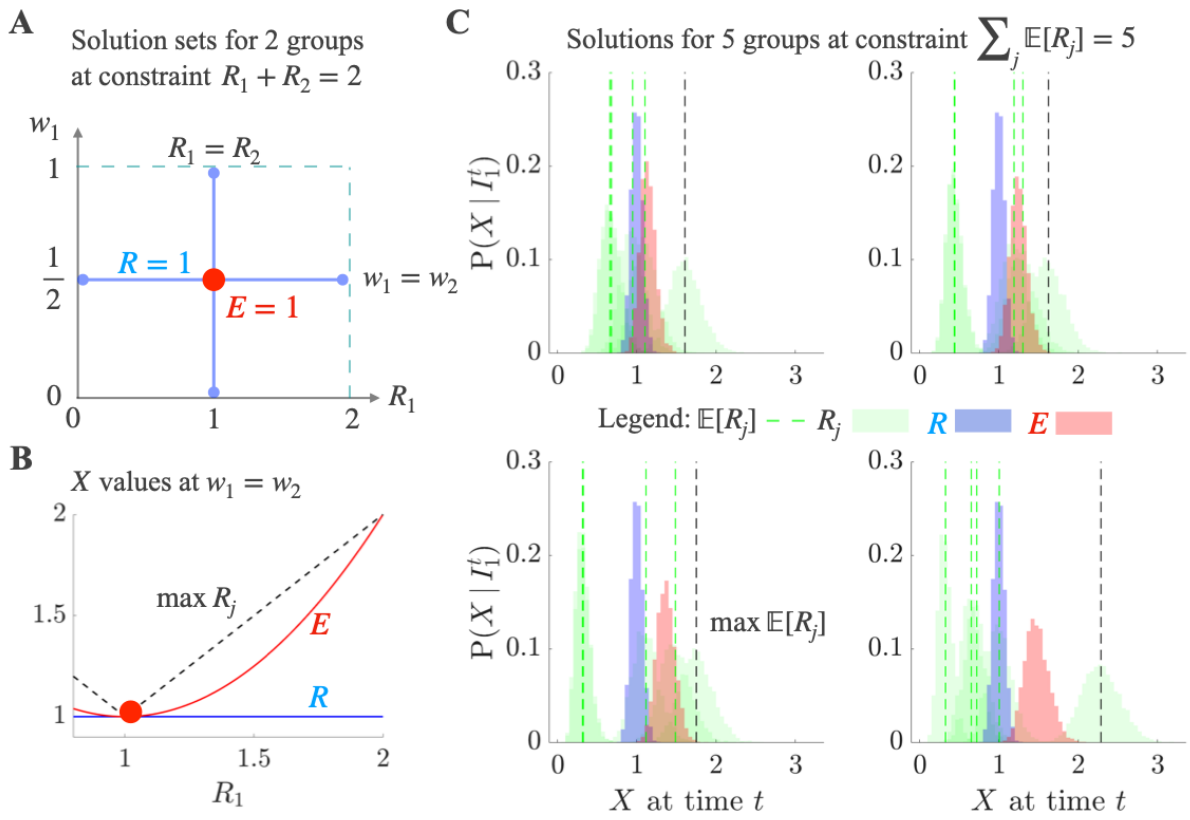

Fig 1: **Space of $R = 1$ and $E = 1$ solutions for varying group reproduction numbers R_j.** **A**: for $p = 2$ groups, we consider R_1 (x-axis) and its weight w_1 (y-axis). Weights sum to 1 so $w_2 = 1 - w_1$. There are an infinite number of solutions yielding $R = 1$. We sketch the subset of those solutions (blue lines with dots at end) satisfying the constraint $\sum_j R_j = p$, which means the R_j have an arithmetic mean of 1. One solution line sets $R_1 = R_2 = 1$ for all weights and the other sets $w_1 = w_2 = \frac{1}{2}$ for all values of $0 \leq R_1 \leq 2$. This line includes many scenarios in which $R = 1$ hides a resurging group ($R_j > 1$). In contrast, $E = 1$ has a unique solution (red dot) guaranteeing $R_1 = R_2 = 1$. **B**: we plot global statistics X (y-axis) for the subsection of the $w_1 = w_2$ solution line from **A** over which R_1 is resurgent (x-axis). R (blue) is unresponsive to the rising R_1, E (red) indicates resurgence and $\max R_j$ (black dashed) is the most sensitive. **C**: for $p = 5$ groups we sample many possible R_j values (green histograms) from gamma distributions $\mathrm{Gam}\left(I_j, \Lambda_j^{-1}\right)$ with I_j as the new infections at time t and Λ_j as the infectious force.

These use past incidence data from times 1 to t, denoted as I_1^t. The mean of the samples is $\mathrm{E}[R_j]$ (green dashed with the maximum $\mathrm{E}[R_j]$ in black) and we constrain the sum over groups to be 5 (ensuring the arithmetic mean of all $\mathrm{E}[R_j]$ is 1). The subplots, from top left to bottom right, show scenarios with increasing R_j heterogeneity among the 5 groups. We construct histograms for global statistics X from the R_j samples (value of reproduction numbers or X are on the x-axis). Across all subplots, we find that an overall $R = 1$ (blue) conceals several resurging groups, while E (red) exposes these dynamics. The methods for these simulations follows from [2,11] with more details given in the Supplement.

Here we test if group-responsive thresholds such as *E=1*, can offer more meaningful stability indicators than *R=1*. **Fig. 1A** shows that at *p=2*, *E=1* implies $R_1=R_2=1$, collapsing the solution space to a point. **Fig. 1B** plots how a resurgent group $R_1>1$ yields *R=1* but *E>1*. **Fig. 1C** and supplement **Fig. S1** validate the generality of these observations. At larger *p*, we see that $E\to 1$ only if all $R_j \to 1$ i.e., widescale (global) and group (local) stability agree when group dynamics become similar. **Fig. 1C** also underscores that neither $X(0)$ (constrained to 1) nor $X(\infty)$ yield representative thresholds. Importantly, unlike *R*, which signals stability confidently, *E* more accurately reflects group uncertainties and only agrees with *R* if all $R_j=1$.

While the inadequacy of the *R=1* threshold is known for certain network models [7,12], we reveal that its limitations extend to simpler, widely-used models (**Eq. (1)**). Even when total infections are roughly constant, *R* in heterogeneous settings may cause biased projections of growth and misrepresent overall epidemic risk (**Fig. 2)**. We find two consequential scenarios where *R=1* can conceal growth: if the resurgent group (i) is masked by infections from a stable group (**Fig. 2B**) or (ii) counteracts a group with declining infections (**Fig. 2C**). Such scenarios are common in practice [6–8] and make *R* a lagging indicator of exponential growth. Hence, policy decisions informed by *R=1* are at risk of being mistimed and inefficient [13].

Crucially, group-responsive reproduction numbers like *E* may better forecast the qualitative impact of time-varying, resurging groups as in **Fig 2B-C**. Moreover, if the epidemic is genuinely stable (**Fig. 2A**), we recover *E=R=1*. Consequently, experimentally designed statistics provide more meaningful stability thresholds, exposing dynamics that are obscured by *R*. However, these benefits require identifying the key heterogeneous groups. While grouping by spatial or location-based features is possible (provided data are collected at those scales), it is hard to disaggregate groups by immunity levels, behaviour or other less conspicuous heterogeneities.

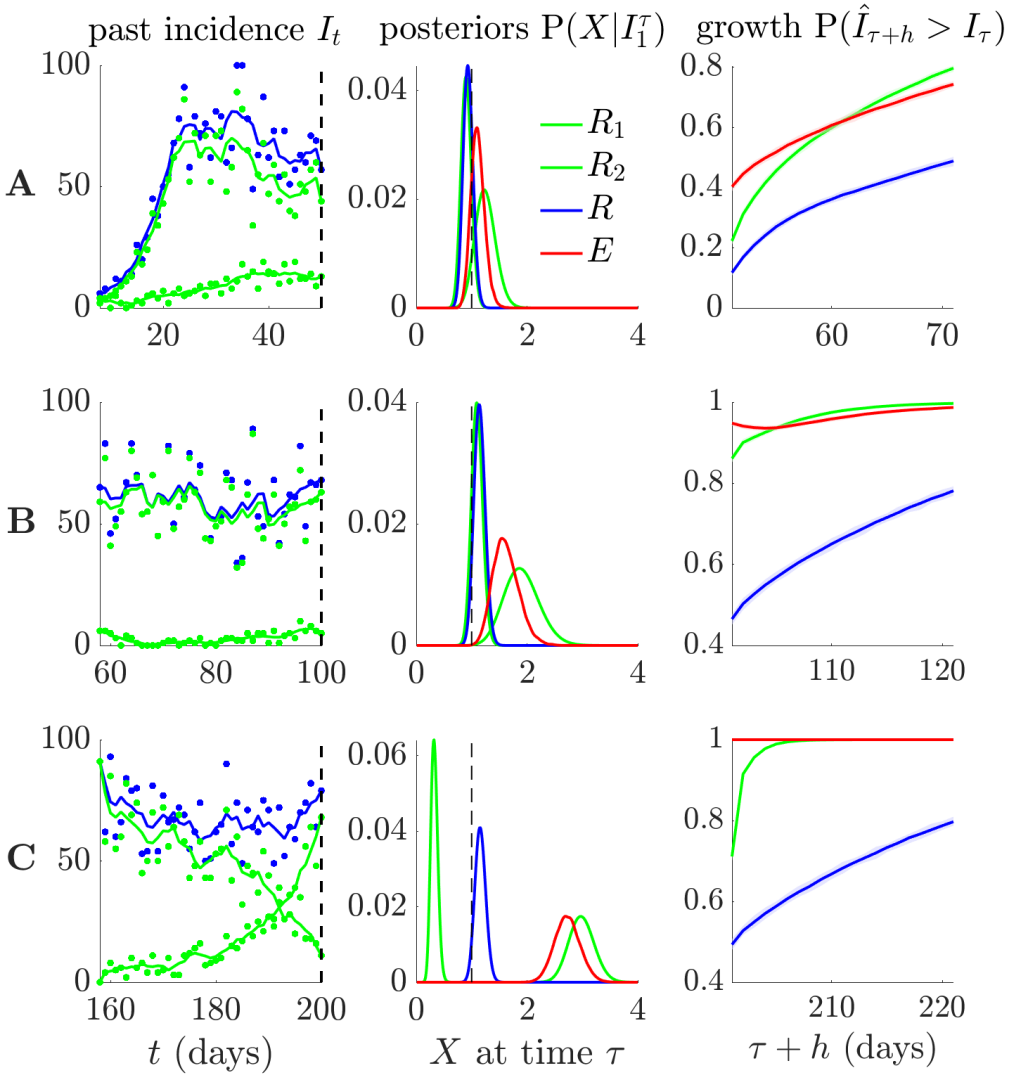

Fig 2: **Growth projections from diverse scenarios with $R = 1$.** We simulate Ebola virus epidemics using renewal models [2] with generation times from [14] for $p = 2$ groups. In scenarios **A-C**, we plot incidence values on the left panels (dots with solid lines as smoothed means) for each group (green) and their sum (blue). Total incidence is approximately stable in all scenarios, but groups display diverse infection patterns. We compute posterior estimates given the past incidence data up to endpoints τ, denoted I_1^τ (central panels) for the group reproduction numbers R_j (green) and resulting global statistics X of the overall (blue) R and risk-averse (red) E reproduction numbers. For all scenarios the posterior of R is approximately 1 (dashed black), concealing salient group resurgences. In the right panels we explore the ramifications of these posterior estimates by computing the growth probabilities that incidence projections over a horizon h, $\hat{I}_{\tau+h}$ will be larger than past incidence (averaged across the last half-week from τ). Group-based projections (green), obtained by summing the local incidence

projected from each group due to their R_j control the expected epidemic dynamics. These dynamics are more reliably signalled at coarse scales by projections from E (red) than from R (blue) (these both use total incidence (blue) from the left panels). We derive all estimates from the EpiFilter package [15] with ribbons representing 95% credible intervals. Full computational details are in the Supplement, including time-series of the posterior X estimates in **Fig. S2**.

Stability thresholds are fundamental benchmarks for implementing or relaxing interventions and pinpointing epidemiologically important shifts. Since these shifts often emerge at group levels, we recommend that response efforts prioritise (a) robustly detecting heterogeneous subgroups within a population (b) estimating transmissibility within those well-mixed groups (to obtain R_j) and (c) merging those estimates into balanced global statistics like E. An $E=1$ more reliably indicates overall epidemic stability and practically achieves what $R=1$, commonly and overconfidently, only estimates theoretically.

Bibliography

1. Anderson R, Donnelly C, Hollingsworth D, Keeling M, Vegvari C, Baggaley R. Reproduction number (R) and growth rate (r) of the COVID-19 epidemic in the UK: methods of. The Royal Society. 2020;
2. Cori A, Ferguson NM, Fraser C, Cauchemez S. A new framework and software to estimate time-varying reproduction numbers during epidemics. Am J Epidemiol. 2013;178: 1505–1512. doi:10.1093/aje/kwt133
3. Cori A, Kucharski A. Inference of epidemic dynamics in the COVID-19 era and beyond. Epidemics. 2024;48: 100784. doi:10.1016/j.epidem.2024.100784
4. The R value and growth rate - GOV.UK [Internet]. [cited 1 Jul 2021]. Available: https://www.gov.uk/guidance/the-r-value-and-growth-rate
5. Green W, Ferguson N, Cori A. Inferring the reproduction number using the renewal equation in heterogeneous epidemics. J R Soc Interface. 2022;19: 20210429. doi:10.1098/rsif.2021.0429
6. Donnat C, Holmes S. Modeling the heterogeneity in COVID-19's reproductive number and its impact on predictive scenarios. J Appl Stat. 2021; 1–29. doi:10.1080/02664763.2021.1941806
7. Li J, Blakeley D, Smith RJ. The failure of R0. Comput Math Methods Med. 2011;2011: 527610. doi:10.1155/2011/527610
8. Backer JA, Wallinga J. Spatiotemporal analysis of the 2014 ebola epidemic in west africa. PLoS Comput Biol. 2016;12: e1005210. doi:10.1371/journal.pcbi.1005210
9. Dalziel BD, Lau MSY, Tiffany A, McClelland A, Zelner J, Bliss JR, et al. Unreported cases in the 2014-2016 Ebola epidemic: Spatiotemporal variation, and implications for estimating transmission. PLoS Negl Trop Dis. 2018;12: e0006161. doi:10.1371/journal.pntd.0006161
10. Parag KV, Obolski U. Risk averse reproduction numbers improve resurgence detection. PLoS Comput Biol. 2023;19: e1011332. doi:10.1371/journal.pcbi.1011332
11. Parag KV, Donnelly CA. Fundamental limits on inferring epidemic resurgence in real time using effective reproduction numbers. PLoS Comput Biol. 2022;18: e1010004. doi:10.1371/journal.pcbi.1010004
12. May RM. Network structure and the biology of populations. Trends Ecol Evol (Amst). 2006;21: 394–399. doi:10.1016/j.tree.2006.03.013
13. Morris DH, Rossine FW, Plotkin JB, Levin SA. Optimal, near-optimal, and robust epidemic control. Commun Phys. 2021;4: 78. doi:10.1038/s42005-021-00570-y
14. Van Kerkhove MD, Bento AI, Mills HL, Ferguson NM, Donnelly CA. A review of epidemiological parameters from Ebola outbreaks to inform early public health decision-making. Sci Data. 2015;2: 150019. doi:10.1038/sdata.2015.19
15. Parag KV, Cowling BJ, Donnelly CA. Deciphering early-warning signals of SARS-CoV-2 elimination and resurgence from limited data at multiple scales. J R Soc Interface. 2021;18: 20210569. doi:10.1098/rsif.2021.0569

Code and Data Availability

We provide MATLAB code to reconstruct the figures at https://github.com/kpzoo/stabilityR.

Funding

KVP acknowledges funding from the MRC Centre for Global Infectious Disease Analysis (reference MR/X020258/1), funded by the UK Medical Research Council. This UK-funded grant is carried out in the frame of the Global Health EDCTP3 Joint Undertaking. UO was supported by a grant from Tel Aviv University Center for AI and Data Science 417 (TAD) in collaboration with Google, as part of the initiative of AI and DS for social good. The funders had no role in study design, data collection and analysis, decision to publish, or manuscript preparation. For the purpose of open access, the author has applied a ‘Creative Commons Attribution’ (CC BY) licence to any Author Accepted Manuscript version arising from this submission.